Available online at www.sciencedirect.com
SCIENCE DIRECT
Surface & Coatings Technology 200 (2005) 62–67
SURFACE & COATINGS TECHNOLOGY
www.elsevier.com/locate/surfcoat

Modeling of gas discharge plasmas: What can we learn from it?

Annemie Bogaerts*, Kathleen De Bleecker, Ivan Kolev, Myriam Madani

University of Antwerp, Department of Chemistry, Universiteitsplein 1, B-2610 Wilrijk-Antwerp, Belgium

Available online 19 March 2005

Abstract

This paper describes some of our modeling efforts for gas discharges, used for plasma surface engineering applications. Depending on the application, we use either a fluid approach or particle-in-cell—Monte Carlo (PIC—MC) models to simulate the plasma behavior. The examples shown in this paper include fluid modeling for nanoparticle formation in silane discharges and for nitrogen dielectric barrier discharges, as well as PIC—MC simulations for a magnetron discharge.

PACS: 52.65.-y
Keywords: Plasma; Gas discharge; Modeling; Fluid model; PIC—MC model

1. Introduction

Gas discharges are used in a range of application fields, such as for plasma surface engineering (etching, thin film deposition, surface modification,...), as light sources, lasers, plasma display panels, in analytical spectrochemistry, for biotechnological and environmental applications [1–11]. In our research group, we are developing numerical models for obtaining better insight in the plasma processes and in plasma–surface interaction, in order to make progress in some of the above-mentioned application fields.

There exist different kinds of modeling approaches to describe gas discharge plasmas, including analytical models [12], fluid modeling [13], the Boltzmann transport equation [14], Monte Carlo [15] and particle-in-cell—Monte Carlo (PIC—MC) [16] simulations, and hybrid models [17]. All these different models have their specific advantages and disadvantages, and are particularly useful for certain conditions. Among these different models, the fluid approach and PIC—MC simulations are the most widely used in literature. Fluid models are particularly useful to describe the plasma chemistry, i.e., when a large number of different species and reactions are taken into account. However, they assume that the plasma species are more or less in equilibrium with the electric field, which means that the energy they gain from the electric field is more or less balanced by the energy loss due to collisions, so that they can be treated as a "continuum" (fluid), and their collective behavior can be described by conservation equations. This assumption is not always true, especially at low gas pressure. PIC—MC simulations, on the other hand, take the non-equilibrium behavior of the plasma species correctly into account, and hence, are more suitable for low gas pressure. They are, however, very time-consuming, especially if a large number of different plasma species is to be considered. In this paper, we illustrate two fluid models and one PIC—MC simulation for describing the plasma behavior in three different types of discharges. It is worth to mention that we also study the plasma–surface interaction in our research group, by molecular dynamics (MD) simulations. However, due to the limitation of space, we only focus here on the modeling of the plasma behavior. More information on our MD simulations can be found in Refs. [18,19].

2. Fluid modeling

A fluid model is based on the moments of the Boltzmann transport equation (i.e., continuity equations of particle

* Corresponding author.
E-mail address: Annemie.Bogaerts@ua.ac.be (A. Bogaerts).

0257-8972/$ - see front matter © 2005 Elsevier B.V. All rights reserved.
doi:10.1016/j.surfcoat.2005.02.057

density, momentum density and energy density). For every plasma species incorporated in the model, a continuity equation (i.e., a balance equation, taking into account all different production and loss mechanisms) and a transport equation (which is a modified version of the momentum conservation equation) are taken into account. The transport is based on diffusion for the neutral particles (molecules, radicals) and on diffusion and migration under influence of the electric field for the charged particles (ions, electrons). Further, an energy balance equation is incorporated for the electrons. The other plasma species (i.e., ions, radicals, molecules and atoms) are assumed to be in thermal equilibrium, so that no energy balance equation has to be considered. Finally, all these equations are coupled to Poisson's equation to obtain a self-consistent potential distribution.

2.1. Fluid model for the description of nanoparticle formation in capacitively coupled (cc) radio-frequency (rf) discharges

The formation of nanoparticles (or dust) in plasma discharges has gained increasing interest in recent years [20–26]. On one hand, the presence of dust is considered to be a problem, because it contaminates the substrate (for deposition or etching applications), and in the micro-electronics industry, nanoparticles can cause killer defects. On the other hand, it has become clear in recent years that nanoparticles in plasmas can lead to very interesting applications as well. For instance, film deposition in solar cell applications seems to benefit from the presence of nanoparticles. Indeed, when the latter are incorporated in the deposited films, the resulting, so-called polymorphous silicon thin films have superior electric properties, making this material a good candidate for use in high-efficiency solar cells.

For this purpose, we are developing a fluid model for a cc rf discharge in silane, to understand the mechanisms responsible for nanoparticle growth in the plasma, and to be able to predict at which conditions the nanoparticles can be incorporated in the deposited layer. In a first stage, we have focused on the nucleation phase, and we have described the detailed plasma chemistry, up to the formation of Si_nH_m species with 12 Si atoms [27,28]. This model considers 68 species, including molecules, radicals, (positive and negative) ions and electrons (see Table 1).

Besides SiH_4 molecules in the ground state, also vibrationally excited SiH_4 molecules, i.e., $SiH_4^{(2-4)}$ at 0.113 eV, and $SiH_3^{(1-3)}$, at 0.271 eV, are taken into account. For every saturated silicon hydride molecule Si_nH_{2n+2}, the corresponding Si_nH_{2n+1} radical has to be considered, since H-abstraction is an important reaction in silane plasmas. The silylenes Si_nH_{2n}, which are a reactive form of the silenes, and are characterized by a single bond between the two silicon atoms with two non-bonding electrons, are also included, since their corresponding anions play a role in the cluster growth. While the positive ions are limited to SiH_3^+, $Si_2H_4^+$and H_2^+, the negative ions are extended up to species containing 12 Si-atoms, because they determine the reaction pathway of nanoparticle growth [29]. The reason is that they are confined in the plasma by the positive plasma potential, so that they have a longer lifetime, and can play an important role in chemical reactions. We make a distinction between the silyl anions ($Si_nH_{2n+1}^-$) and the silylene anions ($Si_nH_{2n}^-$), because they correspond to the different sets of radicals.

Fig. 1 shows the calculated density profiles of the various molecules, radicals, positive and negative ions, and electrons, for a cc rf discharge, at a pressure of 40 Pa and a power of 5 W. It is clear that the molecules are uniformly distributed in the plasma (Fig. 1a), whereas the densities of excited molecules, radicals, ions and electrons drop towards the reactor walls (Fig. 1a,b,c,d). Further, it is found that the anion SiH_3^- is the most important primary precursor of the particle formation. Over 90% of the nanoparticle formation proceeds through the silyl anion ($Si_nH_{2n+1}^-$) pathway, starting from SiH_3^-, and only about 10% goes through the silylene anion ($Si_nH_{2n}^-$) pathway, starting from SiH_2^-. More details about this model (e.g., importance of various chemical reaction mechanisms, etc) can be found in Ref. [28].

As mentioned above, the cluster growth in our model stops at Si_nH_m species with 12 Si-atoms. In reality, however, the dust formation goes on to larger (nanometer and even micrometer sized) particles, but it is not possible to describe the detailed plasma chemistry for an unlimited number of plasma species. Therefore, the further growth will be calculated with a coagulation model, like described in Ref. [30]. Also the charging of the dust particles [31] and their transport (as a result of different forces: electrostatic, gravity, ion drag, neutral drag and thermoforetic force [23]) need to be described. A good knowledge about the charge of the

Table 1
Overview of the different species incorporated in the fluid model for a SiH_4 cc rf discharge, for describing nanoparticle formation

Molecules	Ions	Radicals	Electrons
SiH_4, $SiH_4^{(2-4)}$, $SiH_4^{(1-3)}$	SiH_3^+, $Si_2H_4^+$	SiH_3, SiH_2	e^-
H_2	H_2^+	H	
	SiH_3^-, SiH_2^-		
Si_2H_6, Si_3H_8, Si_4H_{10}, Si_5H_{12}	$Si_2H_5^-$, $Si_3H_7^-$, $Si_4H_9^-$, $Si_5H_{11}^-$	Si_2H_5,Si_3H_7, Si_4H_9, Si_5H_{11}	
Si_6H_{14}, Si_7H_{16}, Si_8H_{18}, Si_9H_{20}	$Si_6H_{13}^-$, $Si_7H_{15}^-$, $Si_8H_{17}^-$, $Si_9H_{19}^-$	Si_6H_{13}, Si_7H_{15}, Si_8H_{17}, Si_9H_{19}	
$Si_{10}H_{22}$, $Si_{11}H_{24}$, $Si_{12}H_{26}$	$Si_{10}H_{21}^-$, $Si_{11}H_{23}^-$, $Si_{12}H_{25}^-$	$Si_{10}H_{21}$, $Si_{11}H_{23}$, $Si_{12}H_{25}$	
	$Si_2H_4^-$, $Si_3H_6^-$, $Si_4H_8^-$, $Si_5H_{10}^-$	Si_2H_4, Si_3H_6, Si_4H_8, Si_5H_{10}	
	$Si_6H_{12}^-$, $Si_7H_{14}^-$, $Si_8H_{16}^-$, $Si_9H_{18}^-$	Si_6H_{12}, S_7H_{14}, Si_8H_{16}, Si_9H_{18}	
	$Si_{10}H_{20}^-$, $Si_{11}H_{22}^-$, $Si_{12}H_{24}^-$	$Si_{10}H_{20}$, $Si_{11}H_{22}$, $Si_{12}H_{24}$	

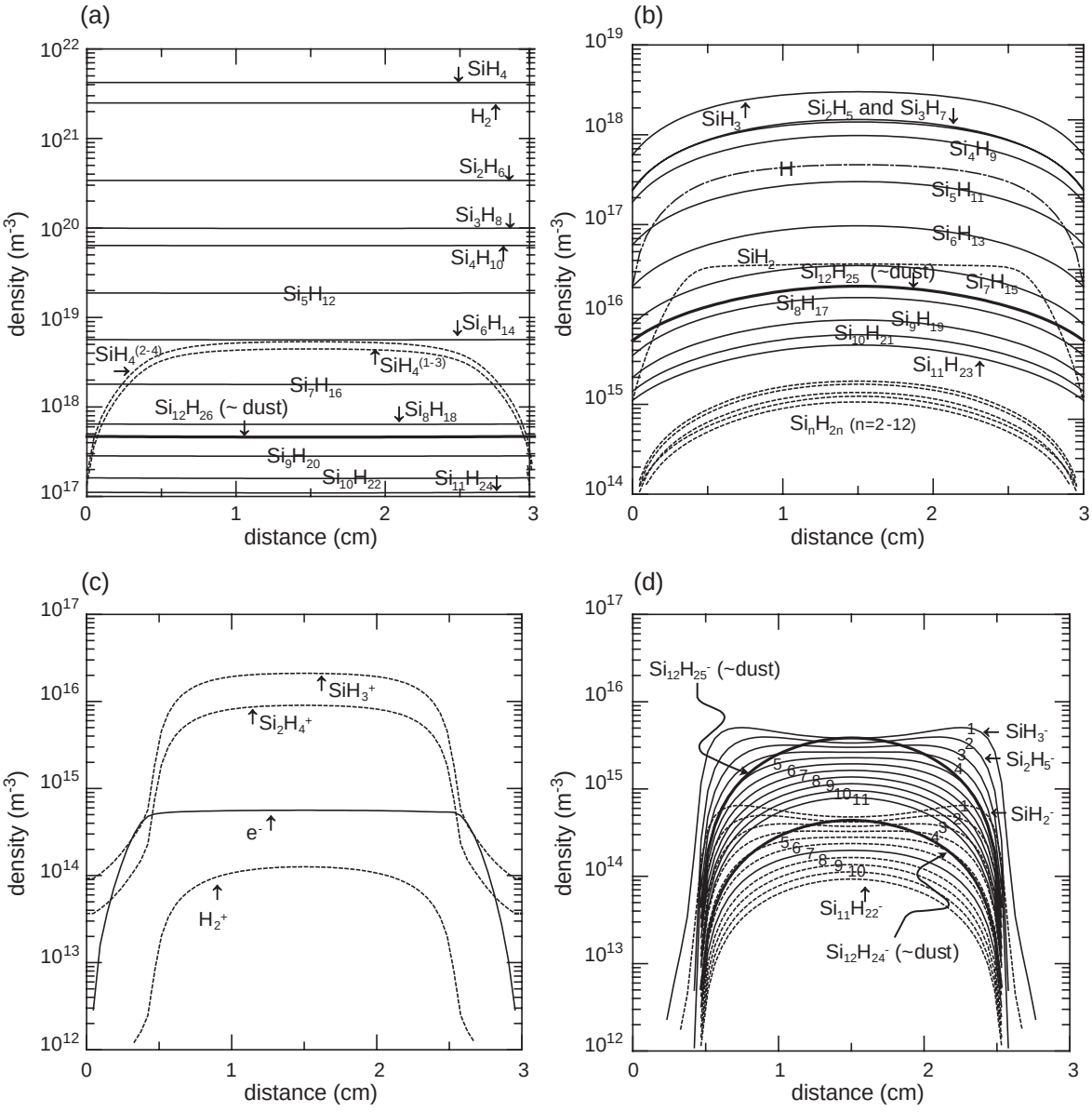

Fig. 1. Calculated time-averaged density profiles of the Si_nH_{2n+2} molecules and the vibrationally excited SiH_4 molecules (a), the silyl radicals (Si_nH_{2n+1}) and the silylenes (Si_nH_{2n}) (b), the positive ions and electrons (c), and the various negative ions (d), for a cc rf discharge in SiH_4, at a pressure of 40 Pa and a power of 5 W. The numbers labelling the curves in Figure 1d correspond to the number of Si-atoms in the anions. Reproduced from Ref. [28] with permission of the American Physical Society.

nanoparticles is very important, because this determines whether the particles can escape the positive plasma potential and reach the surface (and become incorporated in the depositing layer, or contaminate the substrate). This is especially true for the smallest nanoparticles (~few nanometers), because their charge can fluctuate from slightly negative till slightly positive. We have recently developed a model which calculates the charges and forces on nanoparticles of various sizes, ranging from a few nanometers till 100 nm; more information about this model can be found in Ref. [32]. A complete model for the coagulation, coupled to the charging and different forces is under development.

2.2. Fluid model for an atmospheric pressure dielectric barrier discharge in nitrogen

We have also recently developed a fluid model for a dielectric barrier discharge (DBD) in N_2 at 1 atm [33], typically used for deposition and activation of layers [34]. Although it could be argued that DBDs are of extremely transient character, and are non-thermal, non-equilibrium plasmas [8,35], they are generally described by fluid modeling (e.g., [36–39]), which is the most logical choice, because of the high gas pressure. Our fluid model does not describe filament formation in the DBD, but it applies to a stable DBD (i.e., when periodic steady-state is reached),

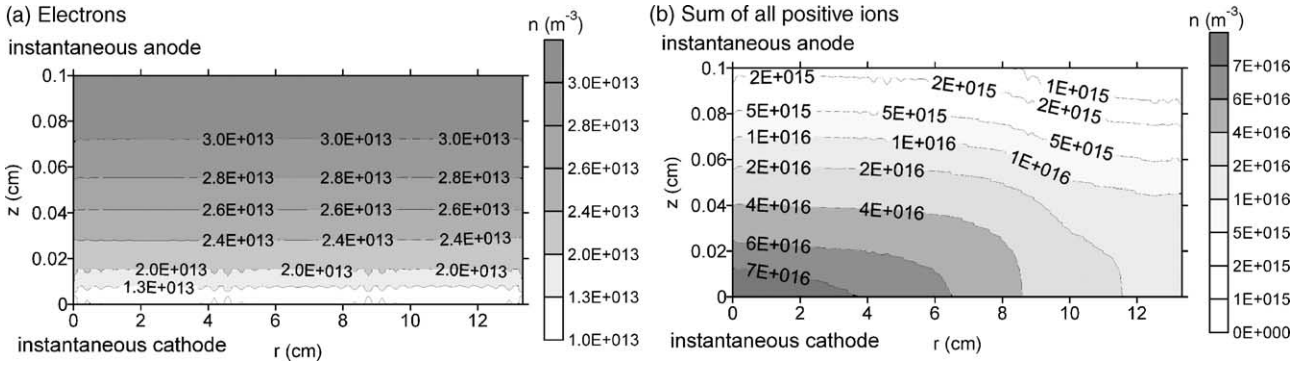

Fig. 2. Calculated 2D density profiles of the electrons (a) and the sum of all positive ions (b), throughout the discharge, at $\omega t = \pi/2$, for a DBD in N_2, with a gap of 1 mm, operating at a frequency of 10 kHz and 10 kV voltage amplitude.

which is the type of discharge required for surface treatment applications. The species taken into account in this model, are: N_2 molecules, N atoms, N_2 molecules in excited states (in the $A\ ^3\sum_u^+$ and $a'\ ^1\sum_u^-$ levels), N^+, N_2^+, N_3^+ and N_4^+ ions.

Beside the usual equations of a fluid model (see above), some additional equations have to be solved in the fluid model for the DBD. Indeed, the DBD consists of two parallel electrodes, and one or both electrodes is covered with an insulating material (dielectric), which needs to be taken into account by using the appropriate boundary conditions for the potential. Moreover, secondary electron emission and electron desorption from the dielectric, when the polarity of the electric field is switched, have to be taken into account as well, by adding two extra terms for the electron flux at the boundary. Hence, this results also in a modified boundary condition for the electron density, compared to a fluid model for a discharge between two conducting electrodes. More details can be found in Ref. [33].

It is well-known that an atmospheric pressure DBD can yield a uniform or a filamentary discharge, and the uniform DBD can be either in glow mode or Townsend mode, depending on the frequency, discharge voltage, width of the discharge gap, the kind of dielectric and its thickness [39]. In the glow mode, the electron and ion densities in the bulk of the discharge are nearly equal to each other, like in a low-pressure glow discharge. In the Townsend mode, on the other hand, the electron density rises from the instantaneous cathode to the instantaneous anode, and the ion density exceeds the electron density by several orders of magnitude, so that there is no charge–neutrality in the plasma [39]. Hence, from the density profiles calculated with our model, we can derive which kind of discharge mode is expected for certain discharge conditions.

Fig. 2 shows the calculated 2D density profiles of the electrons and of the sum of all positive ions, at $\omega t = \pi/2$, for a DBD with a gap of 1 mm, operating at a frequency of 10 kHz and 10 kV voltage amplitude. It is clear that the discharge is fairly uniform in the radial direction, which is good for surface engineering applications. Moreover, the total positive ion density exceeds the electron density by several orders of magnitude, and the electron density rises from the instantaneous cathode towards the instantaneous anode. Hence our model predicts that the DBD is uniform and in the Townsend mode for these particular operating conditions, which is in agreement with literature [38]. We are currently performing a detailed parameter study with our 2D model, to investigate the influence of frequency, applied power and geometry on the structure of the DBD (i.e., uniform vs. filamentary, Townsend vs. glow mode).

3. PIC—MC modeling for a magnetron discharge in argon

Fluid modeling is very useful for describing the detailed plasma chemistry, but it is not so accurate for low gas

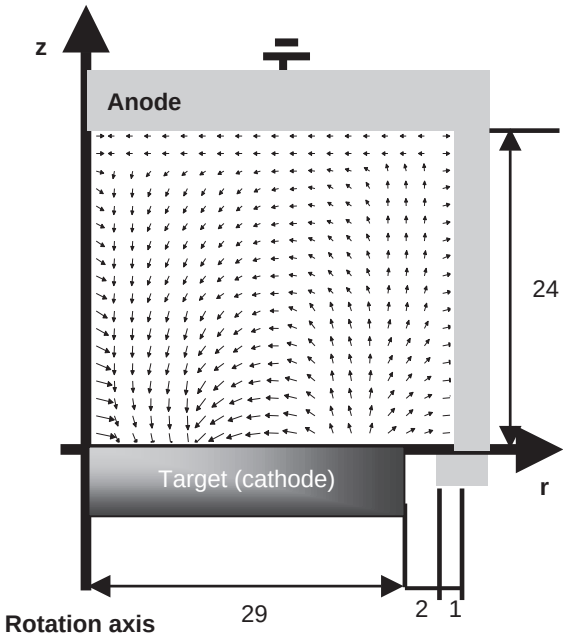

Fig. 3. Magnetron discharge geometry and dimensions, as well as magnetic field lines, used for the calculations. The maximum magnetic field strength, indicated by the longest arrows (i.e., in front of the target, at about 1.8 cm from the cylinder axis), is 300 G. The dimensions are indicated in mm.

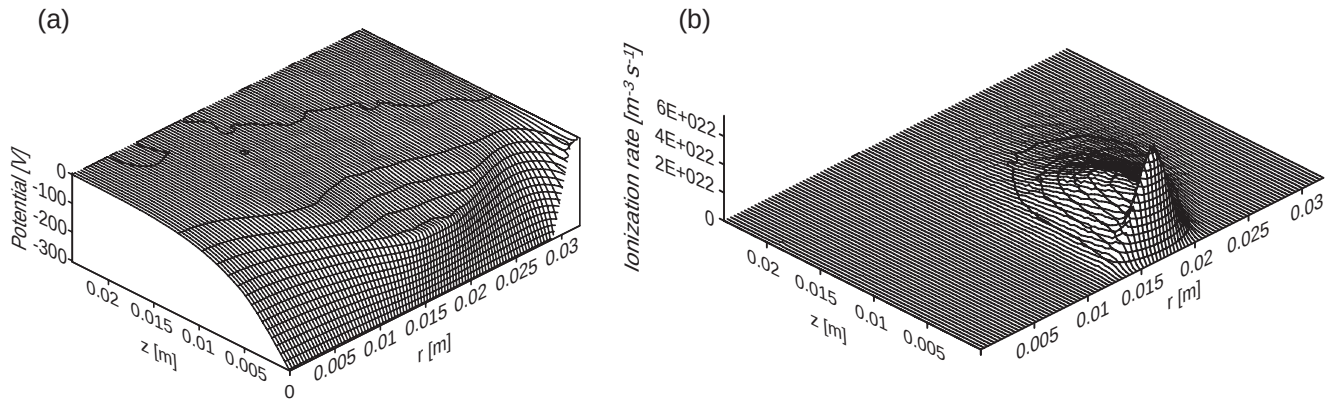

Fig. 4. Calculated potential distribution (a) and electron impact ionization rate (b) in the magnetron discharge shown in Fig. 3, at an argon gas pressure of 4.2 mTorr, a voltage of 350 V, and an electrical current of 250 mA.

pressure, as is typically encountered in magnetron discharges, used for sputter-deposition of thin films. For this purpose, we use PIC—MC simulations, which treat the individual plasma particles, and accurately account for the energy gain from the electric field, and energy losses through collisions [40].

In a PIC—MC model, charged particles (ions and electrons) are replaced by superparticles, with a weight (i.e., number of real particles per superparticle) in the order of 10^7–10^9 (depending on the ion and electron densities). The movement of the superparticles under the influence of the electric field (as well as magnetic field, in our case) is simulated with Newton's laws, during successive time-steps. After each time-step, the charge density is calculated from the particles' coordinates and assigned to the computational grid nodes, on which the Poisson equation is solved. This yields a new electric field on each grid node, which is linearly interpolated to each particle position. Then, the particles are moved again during the next time-step. The collisions (i.e., occurrence of a collision during each time-step, kind of collision and new energy and direction after collision) are treated with random numbers, in the Monte Carlo part of the model.

We have developed a PIC—MC model for a dc planar magnetron discharge, as is shown in Fig. 3. The magnet is placed behind the target, and the magnetic field strengths are indicated with the arrows. The maximum magnetic field strength (cfr. largest arrows in the figure) is found in front of the target, at about 1.8 cm from the cylinder axis. Fig. 4 illustrates the calculated potential distribution (a) and electron impact ionization rate (b). It is clear from this figure that the cathode dark space is shortest, and hence the electric field is strongest, at about 1.8 cm from the cylinder axis, i.e., where the magnetic field strength is at maximum. Also the electron impact ionization rate reaches a maximum in this region, because (i) the electrons gain most energy from the electric field, and (ii) they are trapped in the magnetic field lines. Consequently, also the charged particle (ion and electron) densities reach a maximum in this region. More information about our PIC—MC model for magnetron discharges can be found in Ref. [41].

4. Conclusion

We have shown a few examples of our modeling efforts for gas discharge plasmas, used for plasma surface engineering. Depending on the kind of problem, and discharge operating conditions, either fluid modeling or PIC—MC simulations are employed.

The examples show what kind of information can be expected from numerical modeling. In general, a better insight in the plasma behavior is acquired, which will be helpful for making progress in the application fields.

Acknowledgments

K. De Bleecker acknowledges financial support from IWT. I. Kolev is indebted to the FWO-Flanders for financial support. M. Madani is supported from the Flemish Institute for Technological Research (VITO). The research is also sponsored by the IAP-V program.

References

[1] M.A. Lieberman, A.J. Lichtenberg, Principles of Plasma Discharges and Materials Processing, Wiley, New York, 1994.
[2] A. Grill, Cold Plasma in Materials Fabrication: From Fundamentals to Applications, IEEE Press, New York, 1994.
[3] M. Konuma, Film Deposition by Plasma Techniques, Springer, New York, 1992.
[4] M.G. Abeywickrama, in: J.R. Coaton, A.M. Marsden (Eds.), Lamps and Lighting, Arnold, London, 1997, p. 194.
[5] G.G. Lister, in: H. Schlüter, A. Shivarova (Eds.), Advanced Technologies Based on Wave and Beam Generated Plasmas, NATO Science Series, Kluwer, Dordrecht, 1999, p. 65.
[6] A. Sobel, IEEE Trans. Plasma Sci. 19 (1991) 1032.
[7] C.E. Little, Metal Vapor Lasers, Wiley, Chichester, 1999.
[8] U. Kogelschatz, B. Eliasson, W. Egli, Pure Appl. Chem. 71 (1999) 1819.
[9] T. Hammer, Contrib. Plasma Phys. 39 (1999) 441.
[10] J.R. Roth, D.M. Sherman, R.B. Gadri, F. Karakaya, Z. Chen, T.C. Montie, K. Kelly-Winterberg, IEEE Trans. Plasma Sci. 29 (2000) 56.

[11] A. Bogaerts, E. Neyts, R. Gijbels, J. van der Mullen, Spectrochim. Acta, Part B: Atom. spectrosc. 57 (2002) 609.
[12] Y.T. Lee, M.A. Lieberman, A.J. Lichtenberg, F. Bose, H. Baltes, R. Patrick, J. Vac. Sci. Technol. 15 (1997) 113.
[13] J.D.P. Passchier, W.J. Goedheer, J. Appl. Phys. 73 (1993) 1073.
[14] D. Loffhagen, F. Sigeneger, R. Winkler, J. Phys., D, Appl. Phys. 35 (2002) 1768.
[15] Z. Donko, K. Rozsa, R.C. Tobin, J. Phys., D, Appl. Phys. 29 (1996) 105.
[16] M. Surendra, D.B. Graves, IEEE Trans. Plasma Sci. 19 (1991) 144.
[17] Z. Donko, Phys. Rev., E Stat. Phys. Plasmas Fluids Relat. Interdiscip. Topics 57 (1998) 7126.
[18] E. Neyts, A. Bogaerts, R. Gijbels, J. Benedikt, M.C.M. van de Sanden, Diamond Relat. Mater. 13 (2004) 1873.
[19] E. Neyts, A. Bogaerts, R. Gijbels, J. Benedikt, M.C.M. van de Sanden, Nucl. Instr. Methods B 228 (2005) 315.
[20] A. Bouchoule, in: A. Bouchoule (Ed.), Technological Impacts of dusty plasmas, Dusty Plasmas: Physics, Chemistry and Technological Impacts in Plasma Processing, Wiley, Chichester, 1999.
[21] G.M.W. Kroesen, E. Stoffels, W.W. Stoffels, G.H.P.M. Swinkels, A. Bouchoule, Ch. Hollenstein, P. Roca i Cabarrocas, J.-C. Bertolini, G.S. Selwyn, F.J. de Hoog, Dusty plasmas: fundamental aspects and industrial applications, in: H. Schlüter, A. Shivarova (Eds.), Advanced Technologies Based on Wave and Beam Generated Plasmas, NATO Science Series, vol. 67, Kluwer, Dordrecht, 1999, p. 175.
[22] Ch. Hollenstein, Plasma Phys. Control. Fusion 42 (2000) R93.
[23] W.W. Stoffels, E. Stoffels, Trends Vac. Sci. Technol. 4 (2001) 1.
[24] H. Kersten, H. Deutsch, E. Stoffels, W.W. Stoffels, G.M.W. Kroesen, R. Hippler, Contrib. Plasma Phys. (1988) 41 (2001) 598.
[25] L. Boufendi, A. Bouchoule, Plasma Sources Sci. Technol. 11 (2002) A211.
[26] H. Kersten, R. Wiese, G. Thieme, M. Fröhlich, A. Kopitov, D. Bojic, F. Scholze, H. Neumann, M. Quaas, H. Wulff, R. Hippler, New J. Phys. 5 (2003) 93.
[27] K. De Bleecker, A. Bogaerts, W. Goedheer, R. Gijbels, IEEE Trans. Plasma Sci. 32 (2004) 691.
[28] K. De Bleecker, A. Bogaerts, R. Gijbels, W. Goedheer, Phys. Rev., E Stat. Phys. Plasmas Fluids Relat. Interdiscip. Topics 69 (2004) 056409.
[29] U.V. Bhandarkar, M.T. Swihart, S.L. Girshick, U.R. Kortshagen, J. Phys., D Appl. Phys. 33 (2000) 2731.
[30] U. Kortshagen, U. Bhandarkar, Phys. Rev., E Stat. Phys. Plasmas Fluids Relat. Interdiscip. Topics 60 (1999) 887.
[31] P.K. Shukla, A.A. Mamum, Series in Plasma Physics, IOP Publishing, London, 2002.
[32] K. De Bleecker, A. Bogaerts, W. Goedheer, Phys. Rev., E Stat. Phys. Plasmas Fluids Relat. Interdiscip. Topics 70 (2004) 056407.
[33] M. Madani, A. Bogaerts, D. Vangeneugden, R. Gijbels, J. Appl. Phys., submitted for publication.
[34] O. Goossens, E. Dekempeneer, D. Vangeneugden, R. Van de Leest, C. Leys, Surf. Coat. Technol. 142 (2001) 474.
[35] U. Kogelschatz, Plasma Chem. Plasma Process. 23 (2003) 1.
[36] F. Tochikubo, T. Chiba, T. Watanabe, Jpn. J. Appl. Phys. 38 (1999) 5244.
[37] F. Massines, A. Rabehi, P. Decomps, R. Ben Gadri, P. Ségur, C. Mayoux, J. Appl. Phys. 83 (1998) 2950.
[38] Yu. B. Golubovskii, V.A. Maiorov, J. Behnke, J.F. Behnke, J. Phys., D Appl. Phys. 35 (2002) 751.
[39] Yu.B. Golubovskii, V.A. Maiorov, J. Behnke, J.F. Behnke, J. Phys., D Appl. Phys. 36 (2003) 39.
[40] C.K. Birdsall, A.B. Langdon, Plasma Physics Via Computer Simulations, McGraw-Hill, New York, 1985.
[41] I. Kolev, A. Bogaerts, R. Gijbels, Phys. Rev. E, submitted for publication.